# Integrated cell manipulation system—CMOS/microfluidic hybrid†

Hakho Lee,[ac] Yong Liu,[b] Donhee Ham[b] and Robert M. Westervelt*[ab]

Manipulation of biological cells using a CMOS/microfluidic hybrid system is demonstrated. The hybrid system starts with a custom-designed CMOS (complementary metal-oxide semiconductor) chip fabricated in a semiconductor foundry. A microfluidic channel is post-fabricated on top of the CMOS chip to provide biocompatible environments. The motion of individual biological cells that are tagged with magnetic beads is directly controlled by the CMOS chip that generates microscopic magnetic field patterns using an on-chip array of micro-electromagnets. Furthermore, the CMOS chip allows high-speed and programmable reconfiguration of the magnetic fields, substantially increasing the manipulation capability of the hybrid system. Extending from previous work that verified the concept of the hybrid system, this paper reports a set of manipulation experiments with biological cells, which further confirms the advantage of the hybrid approach. To enhance the biocompatibility of the system, the microfluidic channel is redesigned and the temperature of the device is monitored by on-chip sensors. Combining microelectronics and microfluidics, the CMOS/microfluidic hybrid system presents a new model for a cell manipulation platform in biological and biomedical applications.

## 1. Introduction

Spurred by the significant and rapid advances of microelectronics in the past decades, considerable effort has been directed to miniaturize and integrate analytical devices for chemical and biomedical applications.[1,2] One major outcome of such efforts is microfluidic systems.[3,4] Consisting of microfabricated plumbing networks,[5,6] microfluidic systems can control small volumes of fluids to perform highly sensitive and high-throughput operations in chemical and biological experiments. Microfluidic systems have been successfully demonstrated in various applications including cell sorting,[7] DNA amplifications and separations,[8,9] and chemical synthesis.[10]

We have recently presented a new concept, an IC/microfluidic hybrid system, that further enhances the functionality of microfluidic systems, especially the manipulation capabilities.[11,12] The hybrid system uses integrated circuit (IC) chips as an active, versatile actuator; the IC chips generate local electric or magnetic fields to control the motion of micrometre scale objects inside microfluidic channels. The fields can be dynamically changed by programming the IC chips, which allows many different transport operations within a fixed microfluidic system structure. This approach has been validated by manipulating magnetic beads and magnetically-tagged biological cells with hybrid prototypes that generate local magnetic fields.[11,12]

This paper further extends the proposed concept to biological and biomedical applications. Specifically, we report a new set of advanced manipulations of biological cells using a CMOS/microfluidic hybrid system, with emphasis on sustaining biocompatible environments during the operation. The CMOS/microfluidic hybrid system consists of a custom-designed CMOS (complementary metal-oxide semiconductor) chip and microfluidic channels fabricated on top. The CMOS chip, with micro-electromagnets[13–15] implemented on its surface, directly controls the motion of individual biological cells by generating local magnetic fields. Biological cells are labeled with magnetic beads to be attracted to magnetic fields.[16,17] The microfluidic channels provide a pathway to introduce cells to the chip, and maintain biocompatible environments. To further help maintain biocompatibility, on-chip temperature sensors are integrated to monitor temperature during experiments. The hybrid system can manipulate individual biological cells with microscopic resolution and in parallel fashion. A protocol that exploits the programmability and the speed of the CMOS chip is used to facilitate the chip operation and to bolster biocompatibility.

The unique combination of microelectronics and microfluidics in the CMOS/microfluidic hybrid system presents a new model of a multifunctional microfluidic system for biological and biomedical applications. With CMOS chips functioning as an active component, a hybrid system can perform different, customized tasks just by reprogramming the instructions to the chip, not changing the physical structure of the device. Thus, the hybrid system can serve as a universal platform for a lab-on-a-chip system. Furthermore, by integrating control electronics in the same CMOS chip, a hybrid system can readily provide, for example, parallel operations, multiplexing, and user-friendly interfaces that are now common features in microelectronics. Well-established, standard

[a]Department of Physics, Harvard University, Cambridge, MA 02138, USA. E-mail: westervelt@deas.harvard.edu
[b]Division of Engineering and Applied Sciences, Harvard University, Cambridge, MA 02138, USA
[c]Center for Molecular Imaging Research, Massachusetts General Hospital, Harvard Medical School, Charlestown, MA 02129, USA
† The HTML version of this article has been enhanced with additional colour images.

integrated circuit technology also enables the high-volume production of the chip, which will ensure the consistency in device performances and considerably bring down the cost of the device.

## 2. CMOS IC architecture

The CMOS chip for cell manipulation is designed to generate multiple, localized magnetic field peaks on its surface by using an array of surface microcoils. Magnetic manipulation is chosen for two major reasons: (1) magnetic fields are biocompatible and (2) the fields are not influenced by the medium, ensuring high selectivity of magnetically-tagged cells. Generating multiple magnetic peaks is desirable to control the positions of many individual cells in parallel, which can be used, for example, to study intercellular communications and to assemble artificial cellular structures.

Fig. 1 shows the functional diagram and the micrograph of the implemented CMOS chip. The chip is fabricated in standard CMOS technology (0.18 μm process of Taiwan Semiconductor Manufacturing Company, Taiwan). The chip contains both analog and digital circuits. The analog circuits include 8 × 8 microcoil arrays that generate magnetic field patterns for cell manipulation, a variable 8-step current source for the arrays, and on-chip temperature sensors to measure local temperature of the chip. As the digital part, the row/column decoders choose a specific microcoil in an array and the FET (field-effect transistor) switch networks control the direction and the magnitude of the electrical current in the selected microcoil. The digital circuits facilitate the operation of the chip by reducing the number of external inputs for chip control. In total, ten synchronous external inputs are required to operate an 8 × 8 microcoil array; six signals to address individual microcoils, three to set the magnitude of the electrical current in a microcoil, and one to choose the direction of the current.

Fig. 1B shows the die micrograph of the CMOS chip. The lateral size of the chip is 2 mm × 5 mm, and the supply voltage is $V_{dd}$ = 3.3 V. The chip contains five microcoil arrays with slightly different structures; only one array is enabled during experiments. Fig. 1C shows the close-up of one of the microcoil arrays. The array consists of 64 identical microcoils arranged in 8 rows and 8 columns. The outer diameter of the microcoil is 20 μm and the center-to-center distance between two adjacent coils is 21 μm. To accurately monitor the temperature during the cell manipulation, on-chip temperature sensors are placed in the vicinity of the microcoil array.

### Microcoil design

Several goals have to be met in the microcoil design: (1) the final design should conform to the rules set by the semiconductor foundry, (2) to increase the trapping accuracy, a single peak in the magnetic field magnitude should be generated at the center of a microcoil on the chip surface, and (3) the field magnitude should be maximized to exert more trapping force on the manipulation target.

To meet these goals, the following steps are applied when laying out the microcoil structure. [Step 1] The outer diameter of the microcoil is chosen to be similar to the size of biological
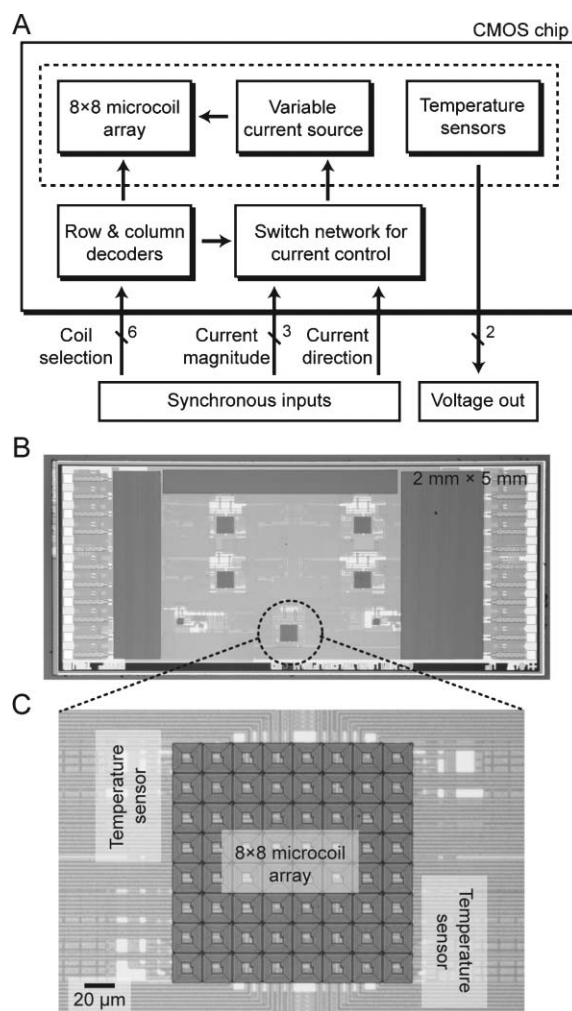


**Fig. 1** Block diagram and micrographs of the CMOS chip for cell manipulation. (A) The CMOS chip contains both analog and digital circuits. Analog circuits (inside the dotted box) include 8 × 8 microcoil arrays, a current source to the arrays, and temperature sensors. Digital logic circuits, decoders and switch networks, control the array by choosing a specific microcoil and setting the direction and the magnitude of the current in the selected microcoil. Digital circuits considerably simplify the interface to the CMOS chip; only ten synchronous inputs are required to individually control 64 microcoils. The temperature sensor output voltages are proportional to local temperature near the array. (B) Die micrograph of the CMOS chip. The chip has a footprint of 2 × 5 mm², and contains five microcoil arrays. Only one microcoil array is activated during operation. (C) Close-up photo of an 8 × 8 microcoil array. The outer diameter of a microcoil and the center-to-center pitch between two adjacent microcoils are 20 μm and 21 μm, respectively. Temperature sensors, implemented on the substrate level, are placed near the array.

cells to be manipulated. This condition facilitates a single cell trapping by each microcoil. [Step 2] Once the diameter is determined, the number of turns in a microcoil is varied to generate a single magnetic field peak, with the maximum magnitude on the chip surface. To have multiple-turn coils, the width of the metal lines is set to the minimum value available from the fabrication process. Note that the metal width determines the maximum current ($I_{max}$) flow in a microcoil. [Step 3] The magnetic field patterns are then calculated using

finite element simulation software (MAXWELL 3D, Ansoft, PA, USA). The result is used to check if the magnitude of the magnetic field is greater than the target value (30 G in the current chip) with the current flow of $0.5I_{max}$. Otherwise, Steps 2 and 3 are repeated. [Step 4] Finally, interconnections between the microcoil and other circuits are made in the metal layer farthest away from the chip surface to minimize stray magnetic fields.

Fig. 2A shows the schematic and the micrograph of the microcoil implemented in the CMOS chip. Three metal layers (the top, the second, and the third, counting from the chip surface) are used, with each metal layer containing a planar coil. The width of the metal line is 1 μm, which can sustain a continuous current of up to ~70 mA. To form a microcoil, the planar coils are connected by vias in series. Adjacent metal layers are separated by a 1 μm thick $SiO_2$ layer, and the top surface of the chip is passivated with a 2.5 μm thick polyimide layer. Fig. 2B shows the calculated magnetic field profiles across the microcoil and on the chip surface. Because most of the contribution to the field magnitude comes from the planar coil in the top metal layer, this planar coil has multiple turns to generate stronger magnetic fields with less current. Planar coils in the second and the third metal layers are primarily used to shape a single peak in the magnetic field magnitude at the center of the microcoil on the chip surface.
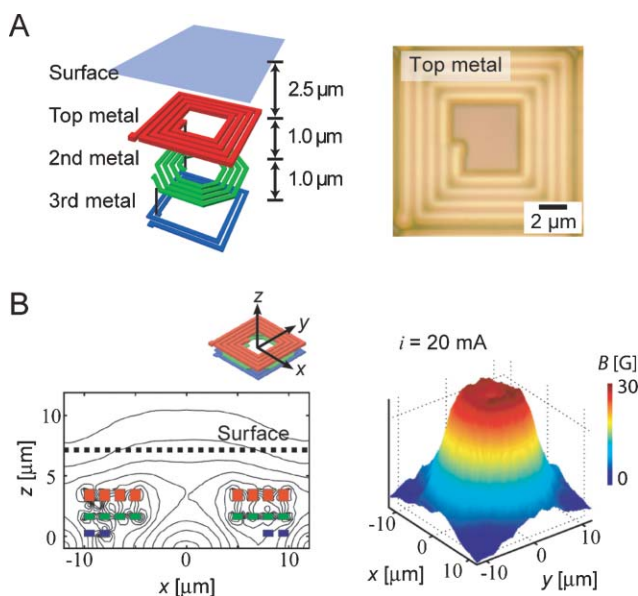


**Fig. 2** Design and magnetic field profiles of a microcoil. The microcoil is designed to generate a single peak in the magnetic field magnitude at its center. (A) The structure of a microcoil. Three planar coils, with each coil in a different metal layer, are connected by vias to form a microcoil. The micrograph shows the planar coil in the top metal layer. The metal lines have the width of 1 μm, and the separation between metal lines is 0.5 μm. Strong magnetic fields can be generated with less current by having a multiple-turn planar coil in the top metal layer. The primary function of the planar coils in the second and the third metal layers is to shape a single peak in the field magnitude. (B) Calculated magnetic field profiles across the microcoil and on the surface of the CMOS chip. A single peak is formed on the chip surface at the center of the microcoil.

## Digital control circuit

To provide an independent control on the electrical current in each microcoil, the CMOS chip integrates multiplexing circuitry that includes row/column decoders, logic gates and switching networks. The details of the circuitry are reported previously[12] and are included here for review. Fig. 3A shows the schematic of the control circuit. The components inside the frame are repeated for each microcoil; the decoders and the on-chip current source are shared in a microcoil array. When the FET switch ($S_c$) is activated by the decoder outputs, the microcoil is connected to the on-chip current source. Note that only one microcoil in an array can access the current source at any given moment. The current source can sink up to 20 mA in the increments of 2.5 mA, providing an 8-step control in the
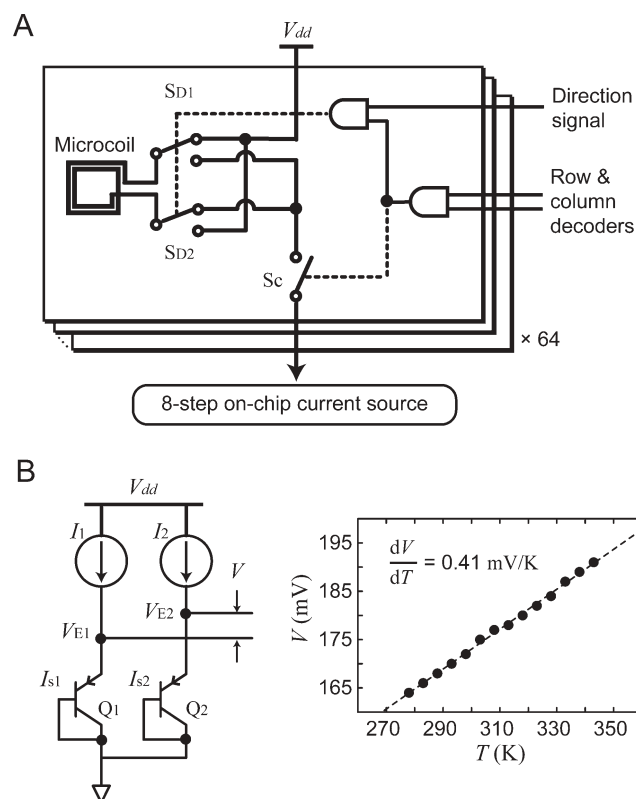


**Fig. 3** (A) Circuit schematic of a microcoil. To enable multiplexing, each microcoil circuit has three FET (field effect transistor) switches and two AND logic gates. The microcoil is connected to the on-chip current source through the switch $S_C$ that is gated by the AND-logic of row and column decoder signals. The current direction is set by the $S_{D1}$ and $S_{D2}$ switches that are controlled by the external direction signal. The on-chip current source provides an 8-step control in the current magnitude with the maximum output of 20 mA. The circuitry inside the frame is repeated for all 64 microcoils; the current source and the decoders are shared in a given microcoil array. (B) Circuit schematic and measured characteristics of the on-chip temperature sensor. The sensor uses two PNP transistors in a diode connection. The emitter voltages ($V_{E1}$ and $V_{E2}$) of the transistors ($Q_1$ and $Q_2$) are directly proportional to absolute temperature. By measuring the difference, $V$, between $V_{E1}$ and $V_{E2}$, errors coming from the variation of the current sources ($I_1$ and $I_2$) can be compensated. Measured output $V$ from the temperature sensor as a function of temperature $T$ shows a good linear relationship with $dV/dT = 0.41$ mV $K^{-1}$.

current magnitude. The direction of the current is set by two FET switches ($S_{D1}$ and $S_{D2}$) that are gated by the external direction signal and the decoder signals. Together with the 8-step current source, the direction control realizes a bipolar, variable current source to each microcoil.

To generate many magnetic peaks for multiple cell trapping, the common current source is shared in the time domain. For example, to create $N^2$ magnetic peaks using an $N \times N$ microcoil array, a current pulse with the duty cycle of $1/N^2$ is sequentially applied to each microcoil, which generates a "flashing" magnetic peak scanning through the array. If the period of the current pulse is smaller than the escape time of a trapped cell due to Brownian motion, the flashing magnetic peak by the current pulse can be averaged as a stationary peak, effectively holding the cell at the same location. Because the estimated escape time of the cells used in this report is >10 s, whereas the minimum pulse period that CMOS chip can handle is <<1 µsec, the current source can be easily shared in the time domain to imitate the simultaneous generation of multiple magnetic peaks. Note that a method in the same principle is employed in optical tweezers to create multiple optical traps from a single light source.[18]

The time-sharing of a current source, together with the multiplexing scheme, brings several advantages, especially when the number of microcoils in an array is large. First, microcoils can still be individually controlled by a small number of external inputs, simplifying the interface to the CMOS chip. Second, because only one microcoil is activated at any given moment, a common current source is sufficient to operate the whole array, making it easier to design and implement the current source. Third, the power consumption in the microcoil array remains nearly constant regardless of the number of microcoils. The heat generation during cell manipulation is minimized, which further enhances biocompatibility of the system.

### Temperature sensors

Regulating the temperature of the hybrid system is an important task during the cell manipulation, as the microcoils generate heat with current flow. To prevent the thermal shock to cells, the temperature of the device should be kept in the physiological range. To monitor local temperature, on-chip temperature sensors are implemented in the vicinity of microcoil arrays. Fig. 3B shows the schematic and the measured characteristics of the on-chip temperature sensor. The sensor is implemented using parasitic PNP bipolar transistors available in a standard CMOS process.[19] With a constant current $I_1$, the emitter voltage $V_{E1}$ in the transistor $Q_1$ is directly proportional to the absolute temperature $T$, $V_{E1} = (k_B T/q)\log(I_1/I_{s1})$, where $q$ is the electron charge, $k_B$ is the Boltzmann constant, and $I_{s1}$ is the leakage current in $Q_1$. Placing another transistor $Q_2$ with an additional current source and by measuring the emitter voltage differences $V = V_{E1} - V_{E2}$, errors coming from the variations of the current sources can be compensated. In the actual chip design, $I_2 = 0.25I_1$ and $I_{s2} = 5I_{s1}$, which gives the relationship $dV/dT = 0.40$ mV K$^{-1}$, where $I_2$ is the current from the additional current source to $Q_2$ and $I_{s2}$ is the leakage current in $Q_2$. The measured sensor output ($dV/dT = 0.41$ mV K$^{-1}$) agrees well with the expected linear dependency.

## 3. CMOS/microfluidic hybrid system

After receiving the CMOS chips from the foundry, microfluidic channels are post-fabricated on top of the IC chips to complete the hybrid system. The microfluidic channels are an essential part of the hybrid system, serving multiple purposes: (1) they provide a pathway to introduce biological cells to the chip surface, (2) microfluidic channels are used to clean and treat the CMOS IC surface before and after experiments, and (3) most of all, microfluidic channels maintain a biocompatible environment during cell manipulation.
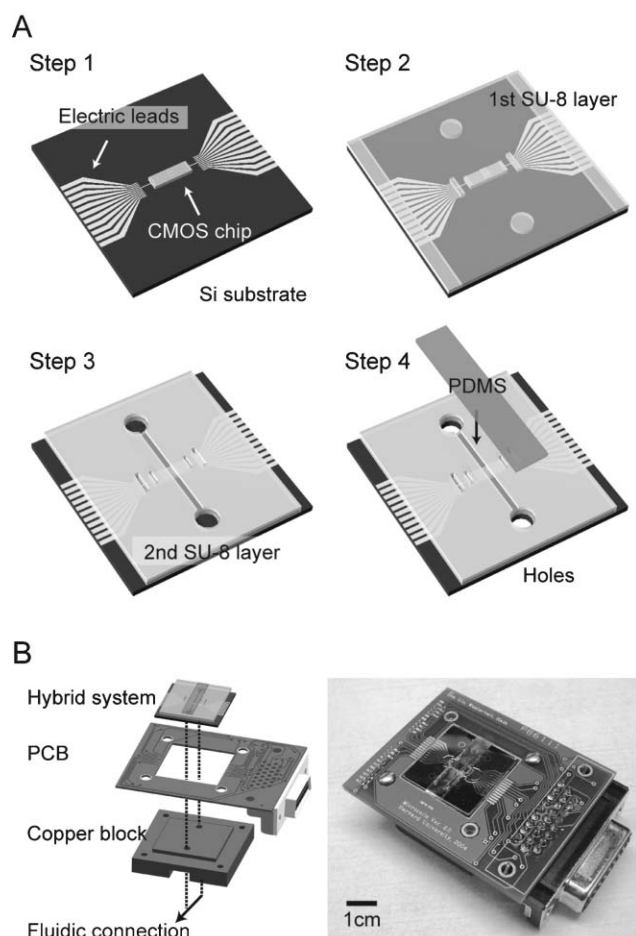
### Fabrication of microfluidic channel

Because the bare CMOS chip has a small footprint (2 mm × 5 mm), the chip is attached to a bigger Si/SiO$_2$ substrate for the subsequent fabrication. The fluidic structure is fabricated using the double layer technique to form microfluidic channels with a uniform depth.[20] This design minimizes the accumulation of cells near the CMOS chip edges during cell injection, reducing the loss of cells.

Fig. 4A illustrates the major steps in the post-fabrication process. [Step 1] First, the chip is glued to a Si/SiO$_2$ substrate with electrical lead patterns. [Step 2] Subsequently, a layer of SU-8 is spin-coated and exposed to UV light to pattern fluidic ports and openings for electrical connections. However, the resist is not developed. The thickness of the first SU-8 layer is comparable to that of the CMOS chip ($\sim$350 µm) to provide a leveled surface. [Step 3] In the next step, a second layer of SU-8 is spin-coated and patterned for a microfluidic channel, and then both SU-8 layers are developed. The resulting microfluidic channel has relatively uniform depth ($\sim$120 µm in the CMOS chip area and 100 µm elsewhere). [Step 4] After hardcuring the SU-8 layers, holes are drilled on the Si/SiO$_2$ substrate to form fluidic inlets, and a thin layer of cured PDMS (polydimethylsiloxane) is placed on top of the SU-8 structure to seal the microfluidic channels.

### System packaging and operation

The assembled hybrid system is packaged for operation as shown in Fig. 4B. The whole system is mounted on a copper stage for cooling, and electrically connected to a printed circuit board (PCB) by wire bonding. Fluidic connections are made from the backside of the hybrid system, which frees the front side from fluidic components. This fluidic connection scheme allows the hybrid system to have a low profile, making it easier to mount the system under a microscope.

The packaged hybrid system is mounted on a microscope stage cooled by a thermoelectric cooler (TEC). Outputs from temperature sensors are used to control a TEC controller (TEC 2000, ThorLabs Inc., NJ) by forming a feedback loop. The temperature of the hybrid system is kept at 10 °C with small variations ($<\pm1$ °C). The manipulation process is observed by a microscope equipped with a CCD camera. To operate the CMOS chip in the hybrid system, a microcomputer board with a microcontroller (ATmega32, Atmel Corporation)

**Fig. 4** (A) Fabrication process of microfluidic channels. [Step 1] The CMOS chip is glued to a Si/SiO$_2$ substrate that has lithographically patterned electrodes. [Step 2] The first layer of SU-8 is spin-coated and patterned, but is not developed. This layer provides a leveled surface for the subsequent microfluidic channel fabrication. [Step 3] The second SU-8 layer is spin-coated and patterned, and both SU-8 layers are developed. The layers are then hard-cured on a hotplate. [Step 4] Holes are drilled on the substrate for fluidic connections and the microfluidic channel is sealed with a cured PDMS (polydimethylsiloxane) layer. (B) Packaging of the CMOS/microfluidic hybrid system. The assembled hybrid system is mounted on a copper block, and is electrically connected to a PCB (print circuit board) by wire bonding. Fluidic connections are made through the backside of the hybrid system, freeing the front side of the system from fluidic tubing components. The packaged system is then mounted on a microscope stage cooled by a thermoelectric cooler.

is custom-made. The microcomputer generates all external control signals to the CMOS chip, and reads out the on-chip temperature sensors.

### Sample preparation

As a representative manipulation target, bovine capillary endothelial (BCE) cells are used. To impart magnetic moment to the cells, peptide-coated magnetic beads are co-cultured with BCE cells, which leads to the uptake of the beads by the cells through endocytosis. Specifically, magnetic beads of diameter 250 nm and with –COOH functional surface group

(PCM-250, Kisker, Germany) are coated with GRGDSP peptide sequence (#22946, AnaSpec, CA) using water-soluble carbodiimide chemistry.[21–23] Bovine capillary endothelial (BCE) cells (CRL-8659, ATCC, VA) are cultured in the presence of the magnetic beads (5 μg ml$^{-1}$) for 24 hours. For the cell manipulation experiments, BCE cells are trypsinized and suspended in PBS (phosphate buffered saline) buffer.

Before introducing the cells, the CMOS chip surface is coated with bovine serum albumin (BSA) by filling the
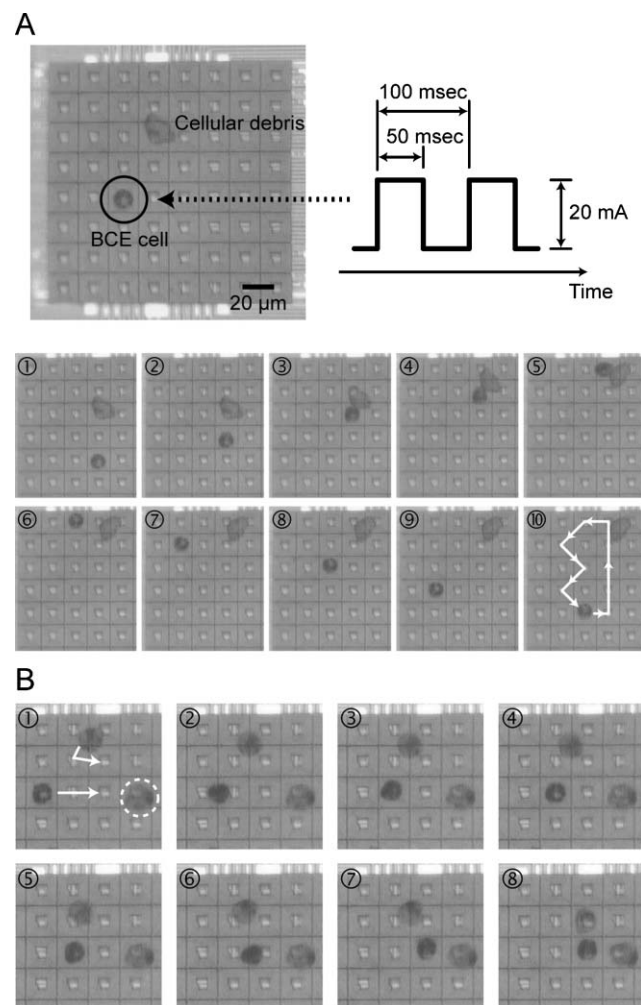


**Fig. 5** Manipulation of BCE (bovine capillary endothelial) cells using the hybrid system. BCE cells are magnetically tagged; magnetic beads of diameter 250 nm are taken up by the cells through endocytosis. (A) A single BCE cell is trapped at the center of a microcoil. A current with the magnitude of 20 mA is pulsed to the microcoil. The period and the duty cycle of the pulse are 100 ms and 50%, respectively. Subsequently, the trapped cell is moved over the microcoil array to make a round trip. The pulse is applied to the microcoil adjacent to the cell, which results in the hopping of the cell from one coil center to another center. (B) Manipulation of multiple cells. Three BCE cells are trapped and independently controlled to sit next to each other; the cell in the dotted circle is held still, and the rest of the cells are moved. The on-chip current source is sequentially shared in the time domain among three microcoils; the current of 20 mA is on for 10 ms and off for 20 ms in each microcoil. Because the diffusion of trapped cells is negligible during the off-time of currents, multiple magnetic traps can be effectively created simultaneously.

microfluidic channel with BSA solution (5% w/v) to suppress unspecific cell binding to the chip surface. Magnetically-tagged BCE cells are then introduced onto the microcoil array through the microfluidic channel. During and after the experiments, the chip surface is cleaned by flushing PBS or distilled water through the microfluidic channel.

## 4. Results and discussion

Experiments with magnetically-tagged cells are performed to demonstrate the several important capabilities of the hybrid system: (1) the control of individual cells with microscopic resolution, (2) the stable trapping and transport of multiple cells while sharing a single current source in time domain, and (3) the dynamic reconfiguration of magnetic fields patterns for versatile cell manipulation.

Fig. 5A shows the trapping and the transport of a single BCE cell using the hybrid system. By applying a current pulse of 20 mA to a microcoil, a magnetic field peak with the magnitude of 30 G is generated, trapping a single cell at the center of the microcoil. The period of the current pulse is 100 ms, with a duty cycle of 50%. Because the diffusion of the cell due to Brownian motion is negligible while the current is off, the cell can be effectively trapped at the same position. To move the cell, the current pulse is applied to an adjacent microcoil, which results in the hopping of the cell from one coil center to another center. The same procedure is repeated to perform a complete round trip of the cell. The manipulation process can be easily reproduced because of the high fidelity operation of the CMOS IC.

To verify the time-sharing of a single current source, multiple cells are simultaneously manipulated as shown in Fig. 5B. Initially, three BCE cells are trapped by sequentially pulsing currents to three microcoils. The period, the duty cycle, and the height of the current pulse are 30 ms, 33%, and 20 mA, respectively. With a single cell held still, the rest of the cells are moved independently by activating appropriate microcoils with the same pulse profile, and finally all cells are arranged next to each other. No cell is lost during this operation, confirming the time-sharing method as an effective way to generate multiple magnetic traps. The capability of the hybrid system to individually control many cells in parallel can be used to conduct many new types of experiments with single-cell level precision. For example, cells of different types can be brought together to study intercellular communications;[24] biological tissues with an artificial cell composition can be assembled by bringing together cells, one-by-one, in a controlled manner.[25,26]

Besides creating magnetic peaks at each microcoil, one can generate more versatile magnetic field patterns by adjusting the magnitude and the direction of currents in microcoils. As an example, Fig. 6 shows how a trapped cell can be positioned at locations other than the centers of microcoils, increasing the spatial resolution of cell trapping. By controlling the current distribution in two adjacent microcoils, a single magnetic peak can be moved in steps less than the center-to-center pitch of the microcoils (Fig. 6A). Note that during the peak movements, the magnitude of the peak remains nearly constant, but the direction of the magnetic field is changing. Fig. 6B shows the step-wise transport of a BCE trapped cell over two
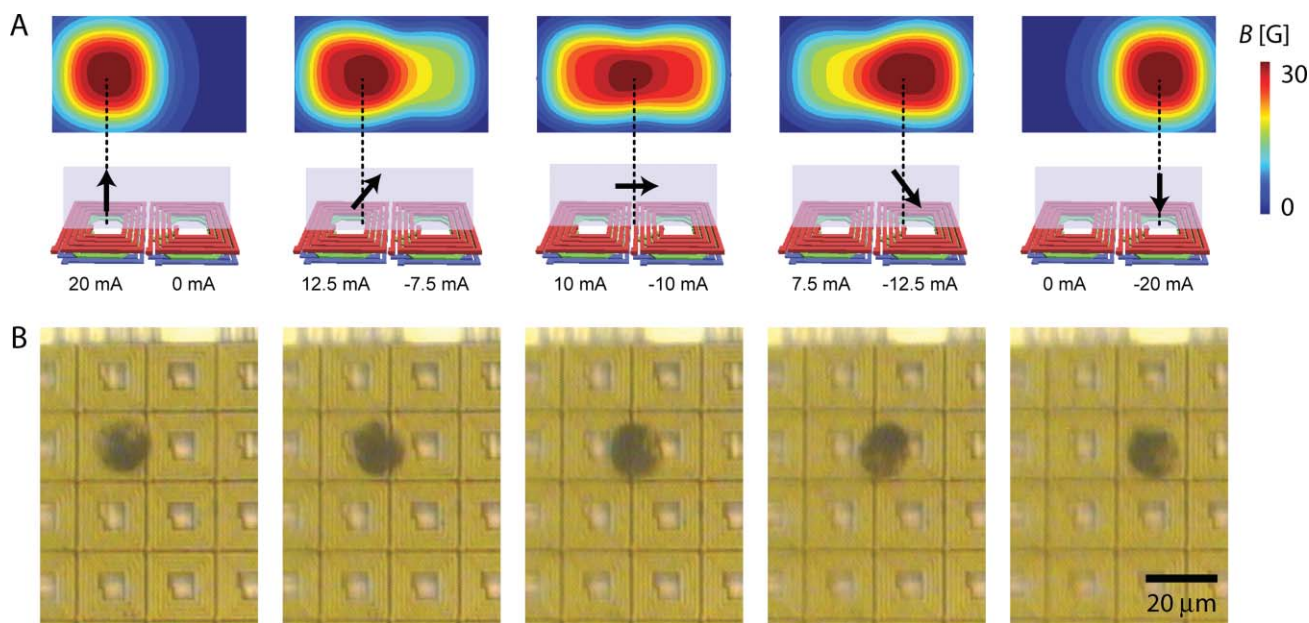


Fig. 6 By controlling currents in the microcoils, many different magnetic field patterns can be generated to provide more flexibility in cell manipulation. As an example, a single peak in the magnetic field magnitude is created and moved in steps over two neighboring microcoils. (A) Calculated magnetic field patterns with current distribution in microcoils. The magnitude of the field peak remains nearly the same, but the direction of the field rotates. The arrows indicate the magnetic field direction in the plane normal to the chip surface. (B) A single BCE cell is trapped and moved using the field pattern in (A). To generate the fields, current pulses with appropriate values and directions are alternatively applied to two neighboring microcoils. The pulse period is 20 ms and the duty cycle is 50%. The cell is observed rolling during the transport due the change of the field direction.

neighboring microcoils. To mimic the magnetic field patterns shown in Fig. 6A, currents of appropriate magnitude and polarity are pulsed to each coil alternatively with a period of 20 ms and a duty cycle of 50%. The trapped cell is observed to roll on the chip surface during the transport, as the direction of the magnetic field is changing at each peak position.

## 5. Conclusions

The CMOS/microfluidic hybrid system presents a new direction for multifunctional microfluidic systems in biological and medical applications. Exploiting the speed and the programmability of the IC chips, the hybrid system brings flexibility inside microfluidic channels. The use of the IC also can bring enhanced robustness,[27] reproducibility and user-interface in microfluidic systems, as happened in consumer electronics. Because the ICs in the hybrid systems are manufactured in conventional semiconductor foundries, mass-production of the system is readily feasible for cost effectiveness. A cheap and disposable hybrid system is especially attractive for medical and clinical uses.

As a proof-of-concept, we have implemented a hybrid prototype that uses a CMOS chip to move biological cells by generating spatially patterned magnetic fields. The motion of individual cells has been controlled at microscopic resolution using microcoil arrays; on-chip temperature sensors and integrated digital circuits facilitate the chip operation, as well as maintaining biocompatible, physiological environments. Because the magnetic patterns can be reconfigured on-demand, the same hybrid system can be used for various purposes with many different cell-types, making the hybrid system a universal cell manipulator. This hybrid system allows one to conduct experiments with single-cell precision in a reproducible fashion, which will be helpful in understanding intercellular processes.

The approach reported here can be applied to implement other types of IC/microfluidic hybrid systems that are dedicated to specific biological and medical applications. For example, hybrid IC/microfluidic chips can be used to sort cells based on dielectrophoresis,[28] to monitor and stimulate electrogenic cells,[29,30] and to detect DNA hybridization.[31] Bringing advanced microelectronics and microfluidics together, the hybrid system will be a powerful lab-on-a-chip platform.

## Acknowledgements

## References

1 P. A. Auroux, D. Iossifidis, D. R. Reyes and A. Manz, *Anal. Chem.*, 2002, **74**, 2637–2652.
2 D. R. Reyes, D. Iossifidis, P. A. Auroux and A. Manz, *Anal. Chem.*, 2002, **74**, 2623–2636.
3 A. Manz, N. Graber and H. M. Widmer, *Sens. Actuactors, B*, 1990, **1**, 244–248.
4 G. M. Whitesides, *Nature*, 2006, **442**, 368–373.
5 M. A. Unger, H. P. Chou, T. Thorsen, A. Scherer and S. R. Quake, *Science*, 2000, **288**, 113–116.
6 T. Thorsen, S. J. Maerkl and S. R. Quake, *Science*, 2002, **298**, 580–584.
7 A. Y. Fu, C. Spence, A. Scherer, F. H. Arnold and S. R. Quake, *Nat. Biotechnol.*, 1999, **17**, 1109–1111.
8 A. T. Woolley, D. Hadley, P. Landre, A. J. deMello, R. A. Mathies and M. A. Northrup, *Anal. Chem.*, 1996, **68**, 4081–4086.
9 J. Han and H. G. Craighead, *Science*, 2000, **288**, 1026–1029.
10 C. C. Lee, G. Sui, A. Elizarov, C. J. Shu, Y. S. Shin, A. N. Dooley, J. Huang, A. Daridon, P. Wyatt, D. Stout, H. C. Kolb, O. N. Witte, N. Satyamurthy, J. R. Heath, M. E. Phelps, S. R. Quake and H. R. Tseng, *Science*, 2005, **310**, 1793–1796.
11 H. Lee, Y. Liu, E. Alsberg, D. E. Ingber, R. M. Westervelt and D. Ham, *Digest of Technical Papers, 2005 IEEE International Solid-State Circuits Conference*, 2005, vol. 1, pp. 80–81.
12 H. Lee, Y. Liu, R. M. Westervelt and D. Ham, *IEEE J. Solid-State Circuits*, 2006, **41**, 1471–1480.
13 C. S. Lee, H. Lee and R. M. Westervelt, *Appl. Phys. Lett.*, 2001, **79**, 3308–3310.
14 H. Lee, A. M. Purdon, V. Chu and R. M. Westervelt, *Nano Lett.*, 2004, **4**, 995–998.
15 H. Lee, A. M. Purdon and R. M. Westervelt, *Appl. Phys. Lett.*, 2004, **85**, 1063–1065.
16 U. Häfeli, *Scientific and clinical applications of magnetic carriers*, Plenum Press, New York, 1997.
17 M. A. M. Gijs, *Microfluid. Nanofluid.*, 2004, **1**, 22–40.
18 K. Visscher, S. P. Gross and S. M. Block, *IEEE J. Sel. Topi. Quantum Electron.*, 1996, **2**, 1066–1076.
19 R. J. Baker, H. W. Li, and D. E. Boyce, *CMOS circuit design, layout, and simulation*, IEEE Press, New York, 1998.
20 J. Carlier, S. Arscott, V. Thomy, J. C. Fourrier, F. Caron, J. C. Camart, C. Druon and P. Tabourier, *J. Micromech. Microeng.*, 2004, **14**, 619–624.
21 S. G. Daniel, M. E. Westling, M. S. Moss and B. D. Kanagy, *Biotechniques*, 1998, **24**, 484–489.
22 J. A. Rowley, G. Madlambayan and D. J. Mooney, *Biomaterials*, 1999, **20**, 45–53.
23 C. Deen, E. Claassen, K. Gerritse, N. D. Zegers and W. J. Boersma, *J. Immunol. Methods*, 1990, **129**, 119–125.
24 P. J. Lee, P. J. Hung, R. Shaw, L. Jan and L. P. Lee, *Appl. Phys. Lett.*, 2005, **86**, 2239021–2239023.
25 S. N. Bhatia and C. S. Chen, *Biomed. Microdev.*, 1999, **2**, 131–144.
26 S. N. Bhatia, M. L. Yarmush and M. Toner, *J. Biomed. Mater. Res.*, 1997, **34**, 189–199.
27 For example, the same CMOS/microfluidic system has been used for >12 months.
28 N. Manaresi, A. Romani, G. Medoro, L. Altomare, A. Leonardi, M. Tartagni and R. Guerrieri, *IEEE J. Solid-State Circuits*, 2003, **38**, 2297–2305.
29 B. Eversmann, M. Jenkner, F. Hofmann, C. Paulus, R. Brederlow, B. Holzapfl, P. Fromherz, M. Merz, M. Brenner, M. Schreiter, R. Gabl, K. Plehnert, M. Steinhauser, G. Eckstein, D. Schmitt-Landsiedel and R. Thewes, *IEEE J. Solid-State Circuits*, 2003, **38**, 2306–2317.
30 F. Heer, S. Hafizovic, W. Franks, A. Blau, C. Ziegler and A. Hierlemann, *IEEE J. Solid-State Circuits*, 2006, **41**, 1620–1629.
31 M. Schienle, C. Paulus, A. Frey, F. Hofmann, B. Holzapfl, P. Schindler-Bauer and R. Thewes, *IEEE J. Solid-State Circuits*, 2004, **39**, 2438–2445.